4. ANALYSIS OF FREJA CHARGING EVENTS

4.1. Background

4.1.1. Why are spacecraft charging studies important ?

The discipline of spacecraft-environment interaction has developed in the past as a series of specific engineering responses to various space environment effects as they were discovered. The variation in current flows to/from a spacecraft in different space environments can cause charge accumulation on the spacecraft surface(s). This charge, in turn, can produce potential gradients between electrically isolated surfaces as well as the spacecraft ground and surrounding space plasma. Spacecraft potentials of several tens of thousands of volts have been reported from several spacecraft (e.g. ATS, DMSP, SCATHA) since their first detection (DeForest, 1972). Such potential buildup can give rise to destructive arc discharges or microarcs that generate electromagnetic noise and erode surfaces. For example, arcing on highly biased solar arrays are so severe that it destroys the array in a short time. The arcing associated with high amplitude surface charging by the magnetospheric plasma is believed to have caused the loss of at least one spacecraft (Shaw et al., 1976) and possibly several more, but also anomalies on several GEO satellites (Rosen, 1976; Leach and Alexander, 1995). This started numerous efforts to understand and mitigate charge accumulation on surfaces in space. The study of charging processes on the Freja satellite is one more such effort.

The natural space environment depends, of course, on exactly where in space the spacecraft traverses. Over the years, several different regions have been identified where high amplitude spacecraft charging is more prone to arise. One such environment is the Polar Earth Orbit (PEO), which traverses the high-latitude auroral plasma regions. Other common charging environments are the Low Earth Orbit (LEO) of cold, dense ionospheric plasma, and the Geostationary Earth Orbit (GEO) immersed in the hot (high-energy) plasmasheet. Charging effects in all of these regions are heavily dependent on the magnetospheric substorm activity level, and therefore on space weather. There are also many (inter-)planetary regions (explored and un-explored) which are known to cause environmental disturbances, especially the magnetospheres of other planets. The Freja measurements, reported here, add further to the knowledge on spacecraft surface charging in a Polar Earth Orbit (PEO). Only very few studies have been devoted to spacecraft charging in PEO (see below), with the exception of the DMSP (Defence Meteorological Satellite Program), which presented an extensive set of surface charging occasions from a lower altitude (840 km).

Modern spacecraft often carry increasingly more complex, sensitive, and expensive payloads, which are affected by the space environment (natural or self-induced). Many instruments have in the past experienced operation problems due to the plasma electrostatic environment, and the interpretation of data from measurements depend critically on the knowledge of spacecraft charging effects. For instance, any shift in potential relative to the spacecraft ground or the space plasma can affect instruments designed to

collect or emit charged particles, but the spacecraft environment may also be a source of instrumental noise in general. Beside destructive arcing effects on surfaces, charge buildup on a spacecraft can in itself attract charge contaminants to sensitive surfaces. This contamination, in turn, can alter the properties of the surface, e.g. changing its conductivity, thermal properties, or optical properties in the case of lenses or mirrors. The study of Freja charging events identifies several problematic payload disturbances, which need to be addressed by instrument designers in the future to assure accurate and scientifically valid data extraction and/or analysis.

4.1.2 Goals of the study of Freja charging events

This chapter summarises the work packages of this project related to the study of charging of the Freja satellite. A detailed analysis of 10 charging events detected by Freja was conducted in order to identify the precise mechanisms behind the charging processes that operate at Freja altitudes (1000–1800 km). The presented events aim at being a representation of different types of charging processes found in the Freja data set. The analysis is complemented with precise electron and ion energy/pitch angle distributions, sunlight/eclipse characteristics, geomagnetic location and auroral activity conditions, as well as cold plasma information.

Five of these events were modelled by the POLAR charging code in order to identify the exact mechanisms behind charging onboard Freja. This analysis also provides a detailed description of the Freja structure and its surface materials. Some recommendations are also given for improvements of the existing charging software tools.

Spacecraft charging was analysed statistically from using all data the Freja spacecraft sampled within the time period October, 1992, to April, 1994 during declining solar activity conditions. This analysis was used to establish the occurrence and intensity characteristics of surface charging events from this polar (high-latitude) orbiting spacecraft in the altitude range 1000–1800 km. The statistics is complemented with information on the environmental characteristics during the charging events, such as cold plasma density, energetic electron and ion distributions, lightning conditions, and geomagnetic location as well as geomagnetic activity.

The detailed database of the Freja charging events is accessible through the SPEE WWW server (http://www.geo.fmi.fi/spee). The database includes all 291 charging events found in the Freja dataset. This database can be used for further studies of surface charging on the Freja spacecraft, but its primary aim is to provide an easy accessible database on environmental statistics for spacecraft charging.

4.2. The Freja satellite and its payload

4.2.1. The Freja mission

The Freja* spacecraft was launched on October 6, 1992, and ended its operations in October, 1996, two years after its planned operation time. Freja was a spin-stabilized sun-pointing spacecraft with a spin period of 6 seconds. The Freja mission objective was to study the polar (high-latitude) auroral processes and the spacecraft was therefore equipped with a highly advanced plasma payload package and the spacecraft itself was designed to be as electrically clean as possible. Such a payload package is, of course, also suitable for spacecraft charging studies. Numerous surface charging events did indeed occur with negative charging levels as large as –2000 V. No damagne were apparently associated to the charging, probably because of the high conductivity of the surface materials (see section 4.5. below). Surface charging should, however, be of concern for low-altitude hihg-inclination spacecraft design.

This study is limited to the time period October, 1992, to May, 1994, when most on-board plasma instruments provided good measurements. This time period covered a declining phase of the solar cycle from medium solar activity to minimum solar activity. The Freja spacecraft orbited Earth with a 63° inclination, with the apogee in the northern hemisphere of 1756 km, and the perigee in the southern hemisphere of 601 km. Freja therefore passed along the auroral region almost tangentially on each orbit, and can therefore be considered to be a Polar Earth Orbit (PEO) spacecraft. Only low-resolution survey data exist from below the altitude of 1000 km.

4.2.2. The Freja payload

The Freja project was designed to give high temporal/spatial resolution measurements of the auroral plasma characteristics and contained 73 kg of state-of-the-art plasma diagnostic experiments. A detailed description of all experiments onboard Freja can be found in a special Freja instrumentation issue of *Space Science Reviews* (Lundin et al., 1994). Here we just note that we have made most use of the F3H, F4, and the F7 instrumentations. The instruments are summarised below.

---

*) ***Freja***, *the goddess of fertility in Nordic mythology, was not a gentle "Afrodite of the north". She was the empress of Folkvang, the estate of the Nordic Gods, and she stood close to Odin, the almighty. She is a female warrior like Pallas Athena in Greek mythology. Her power encompassed life and death, love and battle, fertility and black magic. Half of the heroes killed in battle were her toll, sent to her for her amusement.*

MATE

The MAgnetic imaging Two-dimensional Electron spectrometer (MATE) measured electron energy and angular distributions in the energy range 0.1-100 keV. MATE consisted of a 360° field-of-view sector magnet energy analyser with 90° deflection angle for simultaneous energy and pitch-angle determination. The sampling rate for the full energy range was 10 ms, and a collimator system enabled measurements of the energy spectrum at 16 energies (with resolution $\Delta E/E = 30$ %) and 30 angular sectors.

Unfortunately, the MATE instrument was not deployed completely and was to 1/3 blocked by the Freja spacecraft itself and only every 4th angular sector provided data. Furthermore, the instrument did work properly up to orbits around 1600 only, whereafter only the integrated flux of the high energy electrons (with some pitch-angle information) could be obtained. This instrument was otherwise the only instrument onboard Freja that could give accurate information on the high-energy electrons.

TESP

The Two-dimensional Electron SPectrometer (TESP) on Freja consisted of a "top-hat" style sweeping electrostatic analyzer. The energy range of 20 eV-25 keV was covered by 32 sectors to complete a spectrum. Depending on instrument mode, 16 or 32 spectra were returned each second (31.25 ms resolution). The angular field-of-view was the full 360° and electrons were counted in 32 equally spaced bins, yielding an angular resolution of 11°. The entrance aperture of TESP also contained a set of electrostatic deflectors which allows the plane of acceptance to be "warped" into a cone.

The TESP experiment started working around orbit 720, when the instrument software were sent to the spacecraft after the launch. TESP data cover energies up to 25 keV, but give nontheless important information regarding the high energy electrons. Since low-energy electrons may cause an excess emission of secondary electrons (and thereby stabilize charging), the information from this experiment is very usefull.

TICS

The Three-dimensional Ion Composition Spectrometer (TICS) measured the positive ion distributions in the energy range 0.5 eV/q–5 keV/q. TICS carried out measurements perpendicular to the spacecraft spin plane and thus gave 3D ion measurements every 3 s. TICS consisted of a spherical "top-hat" electrostatic analyser with 16 or 32 energy steps sampled each 10 ms. This means that one 16 step energy sweep took 160 ms + 40 ms for adjusting the high voltage. TICS also gave limited ion composition information in the range 1–40 amu/q. This instrument gave us the best measurement of the degree of negative charging, since the whole ion population was accelerated toward the spacecraft and the whole ion population could be detected at energies corresponding to the potential of the spacecraft. Even as small negative potentials as –5 V can be seen in the TICS data.

Langmuir probes

Freja carried 4 spherical probes (P3-P6), which could be operated in the Langmuir mode, situated on wire booms, and a cylindrical Langmuir probe (CYLP). The CYLP was almost always available, but the operation of the spherical probes depended on measurement mode for the orbit in question. The spherical LPs were 6 cm in diameter and coated with graphite (Dag 213). They were situated 5.5 m (P5 and P6) and 10.5 m (P3 and P4) from the spacecraft respectively. The CYLP is 57 cm long and 1 cm in diameter, and was made of carbon fibre. It was mounted on the DC magnetometer stiff boom (2 m from the spacecraft) parallel to the spin axis. As the spin axis was "sun-pointing" within 30°, this minimised the projected surface area and thus the photoelectron emission.

A Langmuir probe samples all current contributions in a plasma at a certain bias potential, with respect to the spacecraft floating ground, according to its current-voltage characteristics. Therefore, a LP yields a direct measurement of the charge state of the probe (and spacecraft). Most often this measurement gives information on the density and electron temperature of the ambient thermal plasma, since the sampled probe current is directly proportional to $n_e / \sqrt{T_e}$ and since the ambient thermal electron current usually dominates the current collection. However, when the spacecraft (and probe) attains a large negative potential (i.e. a large negative charge) with respect to the surrounding plasma, the thermal electrons start to become repelled from the LP. If the negative potential becomes much larger than the average energy of the thermal electrons (typically below 2 eV), a majority of these electrons cannot easily reach the negatively charged LP, and the probe current drops sharply to very low values more characteristic for the collected ion thermal current. A LP current below $5 \cdot 10^{-8}$ A therefore either indicates a negative charging event of at least a few V negative or a very low electron density below 10^7 m^{-3}. The sampled LP current is therefore a very sensitive measurement for spacecraft charging, even though it does only give a threshold value for the negative potential during charging events.

Plasma wave instruments

The plasma wave experiments (F4) measured in three frequency ranges, LF (5–2000 Hz), MF (5 Hz–16 kHz) and HF (10 kHz–4 MHz). The LF measurements most often consisted of 4 simultaneously sampled waveform components of several possible types and the MF consisted most often of 2 simultaneous waveform components. All wave measurements were normally made in snapshots of various lengths and duty cycle, dependent on sampling rate, telemetry allocations, etc. There were 3 pairs of spherical probes, P12 (21 m), P34 (21 m), and P56 (11 m) mounted on three wire boom pairs in the satellite spin plane. Four of the probes (P3, P4, P5, and P6) could be used for either electric field measurements (potential mode) or plasma density measurements (current mode). Probes P1 and P2 were only used for electric field measurements. The HF measurements were made either with the P12 probe pair or a special short (1.2 m) antenna probe pair (PAB) mounted on one of the magnetometer booms. Freja carried also a Search Coil Magnetometer (SCM) assembly consisting of three identical coils which were mounted orthogonally, one parallel to the spin axis and the other two in the spin plane. All

signals were transmitted to the ground as waveforms and there was no onboard treatment except filtering, A/D conversion and intermediate storage.

During a charging event the LF and MF electric field measurement became strongly disturbed up to rather large frequencies due to large negative potentials of the probes. This is due to the fact that the potential between the spacecraft and each of the probes were measured separately and the total potential between the probes is just the difference between these results. Unfortunately the work point of these measurements only allow for a +/–50 V change, which obviously was exceeded during charging events. The HF measurements on the other hand make use of the short PAB booms and measure the relative difference in potential between these probes directly. Therefore no large disturbances occurred on the HF measurements during charging events.

Magnetometer

The FluxGate Magnetometer (FGM) was mounted on a 2 m long boom, and gave the full 3D vector measurements of the DC geomagnetic field as well as magnetic variations with 128 samples/s. The magnetic fluctuation level was often a good measure of the auroral activity, and the magnetic measurements seemed not to be affected by charging events in any way.

Experiment	***Measurement***	***Principal Investigator***
F1 Electric Fields	3 pair of wire booms (< 3 kHz)	Göran Marklund
F2 Magnetic Fields	3-axis fluxgate magnetometers (< 64 Hz)	Lawrence Zanetti
F3H Hot Plasma	2D electron spectrometer (MATE, 0.1-115 keV) 2D ion composition spectrometer (TICS, 1 eV-10 keV)	Lars Eliasson
F3C Cold Plasma	3D ion/electron distr. (<300 eV)	Brian Whalen
F4 Plasma Waves	3 wire boom pairs, 3-axis search coil magnetometers, HF booms (E, B, dn/n, 1 Hz-4 MHz)	Bength Holback
F5 Auroral Imager	2 UV CCD Cameras	John S. Murphee
F6 Electron Beam	3 electron guns (3D of E-field)	Götz Paschmann
F7 Electron Spectrometer	2D electron spectrometer (TESP, 0.01-20 keV)	Manfred Boehm

4.3. Examples of Freja charging events

4.3.1. Methodology

Several selection criteria are necessary for identification of charging events on the Freja spacecraft in order to distinguish these events from naturally occuring plasma processes

(e.g. transverse ion heating events in connection with plasma density cavities). One very sensitive indicator for negative charging events is that the Langmuir probe (LP) current drops to values below about $5 \cdot 10^{-8}$ A, because very few thermal electrons can reach the negatively charged probe. A strong negative potential of the spacecraft also causes the surrounding ion populations to accelerate toward the spacecraft. The ion spectrometers onboard Freja (e.g. TICS) detected a general increase in energy of all ion components when this happened. This general increase has a different appearance in the data compared to naturally occuring ion heating events, in that a "string" of enhanced flux is detected at all pitch-angles rather than showing conic characteristics. Unfortunately, ion heating events and spacecraft charging events occured simultaneously at times. A third indicator is that the low-frequency electric field measurements became strongly disturbed.

We employ the following methodology when identifying surface charging events on the Freja spacecraft:

1) The sampled Langmuir probe currents of the spherical probes (P3, P4, P5, P6) as well as the cylindrical (CYLP) probe are below $2 \cdot 10^{-8}$ A. This either means that the plasma density is extremly low or the probes are negatively charged to a few V.
2) The narrowband Langmuir emission (in the HF) indicates a larger density than the Langmuir probe currents would indicate. During charging events the narrowband HF emission is often unaffected, while the LP currents drops to very low values, thus suggesting that the density remains larger than the LP current would indicate.
3) The TICS data show a clear lift in energy of the whole ion population at least 5 eV, and the ion distribution characteristics show a well-defined energy "strip" at most pitch angles. If the ion distributions have characteristics similar to transverse ion heating events (ion conics), they are only kept as suspected charging events if there is a clear miss-match between the density inferred from the Langmuir probes and the HF narrowband emissions.
4) The events should show disturbances in the LF and MF electric field data. This is not a requirement for identifying a charging event, though.

4.3.2. Determination of plasma density

The HF measurements of narrowband Langmuir waves, and/or the upper cutoff of electrostatic whistler type waves, give us the best estimate for the electron density from

$$f_{pe} = \frac{1}{2\pi}\sqrt{\frac{n_e e^2}{\varepsilon_0 m_e}} \quad \Leftrightarrow \quad n_e = \frac{\varepsilon_0 m_e}{e^2}\left(2\pi f_{pe}\right)^2$$

The electron density inferred in this way varies most of the time almost exactly as the probe current measured by the LPs. This correlation strongly supports the interpretation that both the narrow-band HF signals and the probe current give the plasma density. However, during surface charging events the sampled LP current drops to very low val-

ues and cannot longer be a good estimate for the plasma density. In such cases the narrowband Langmuir emission (if existing) is a very useful tool for determining the electron density (about 10 % accuracy).

The conversion factors between plasma density and sampled LP currents are based on calibrations against the HF plasma frequency emissions for a statistically significant dataset. The following conversion factors have been obtained (Carlson, 1994):

Probe	**[m^{-3}/A] in Eclipse**	**[m^{-3}/A] in Sunlight**
Spherical Probes	$1.2 \cdot 10^{15}$	$7.5 \cdot 10^{14}$
CYLP	$8.8 \cdot 10^{15}$	$2.1 \cdot 10^{15}$

These conversion factors are accurate to within 95 % confidence.

Another check of plasma density can be gained from the lower frequency cutoff of whistler waves belonging to the dispersion surface connected to the lower hybrid waves. This cutoff usually occurs around a few kHz. During a charging event the MF electric field measurements are strongly disturbed, but the weak magnetic component of the whistler emission (as measured by the SCM) is often sufficient to determine this cutoff. The cutoff occurs near the lower hybrid frequency, given by

$$f_{LH} = \frac{f_{pi}}{\sqrt{1 + f_{pe}^2 / f_{ce}^2}}$$

and is therefore dependent on the ion composition. This cutoff thus gives a rough estimate of the plasma density.

4.3.3. Orbit 790, a typical charging event

Orbit 790 is famous in the Freja community because a well-developed substorm took place during this orbit and several papers have been written about it. However, no one has addressed the charging event that seems to have taken place in the middle of the auroral activity and transverse ion heating. Figure 4.3-1 displays the overview particle data.

Between 0233:00 UT and 0243:00 UT a large auroral disturbance occurred with large fluxes of high-energy electrons as measured by both the TESP instrument (panel 7) and the MATE instrument (panel 5). The ion population was uplifted in energy in the time interval 0234:00–0239:00 UT. Most of this particular time interval occurred during sunlight conditions (panel 4), and only the later part of the event was in eclipse, where most Freja charging events yook place. The first part of the auroral event between 0233:00–0236:00 UT was most probably related to transverse ion heating, since there was no dropout in the LP current during this period. The later part is presented in more detail in Figures 4.3-2 and 4.3-3.

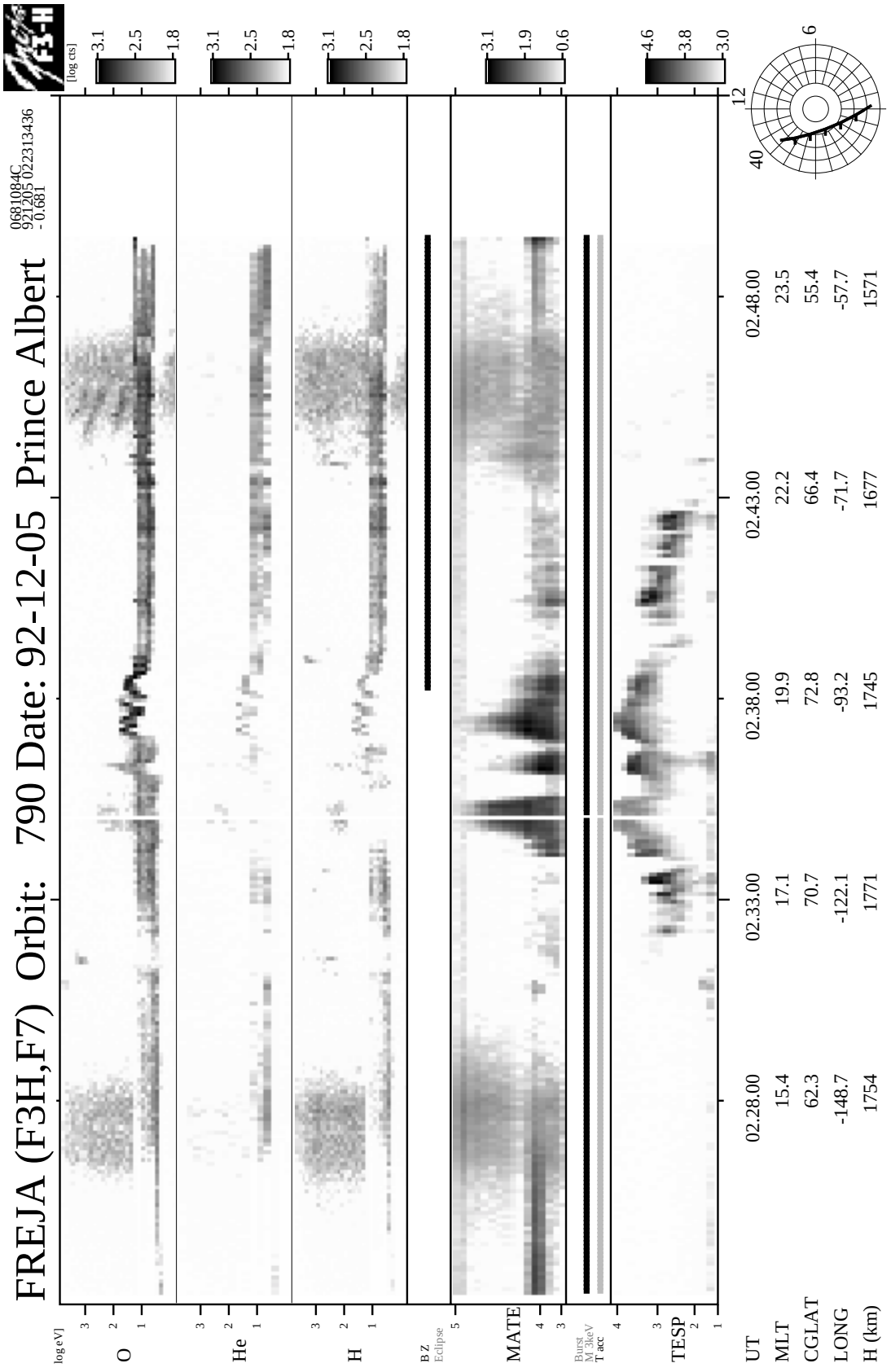

Figure 4.3-1. Overview of orbit 790 particle data. The charging event took place near the terminator at 0238:00 UT.

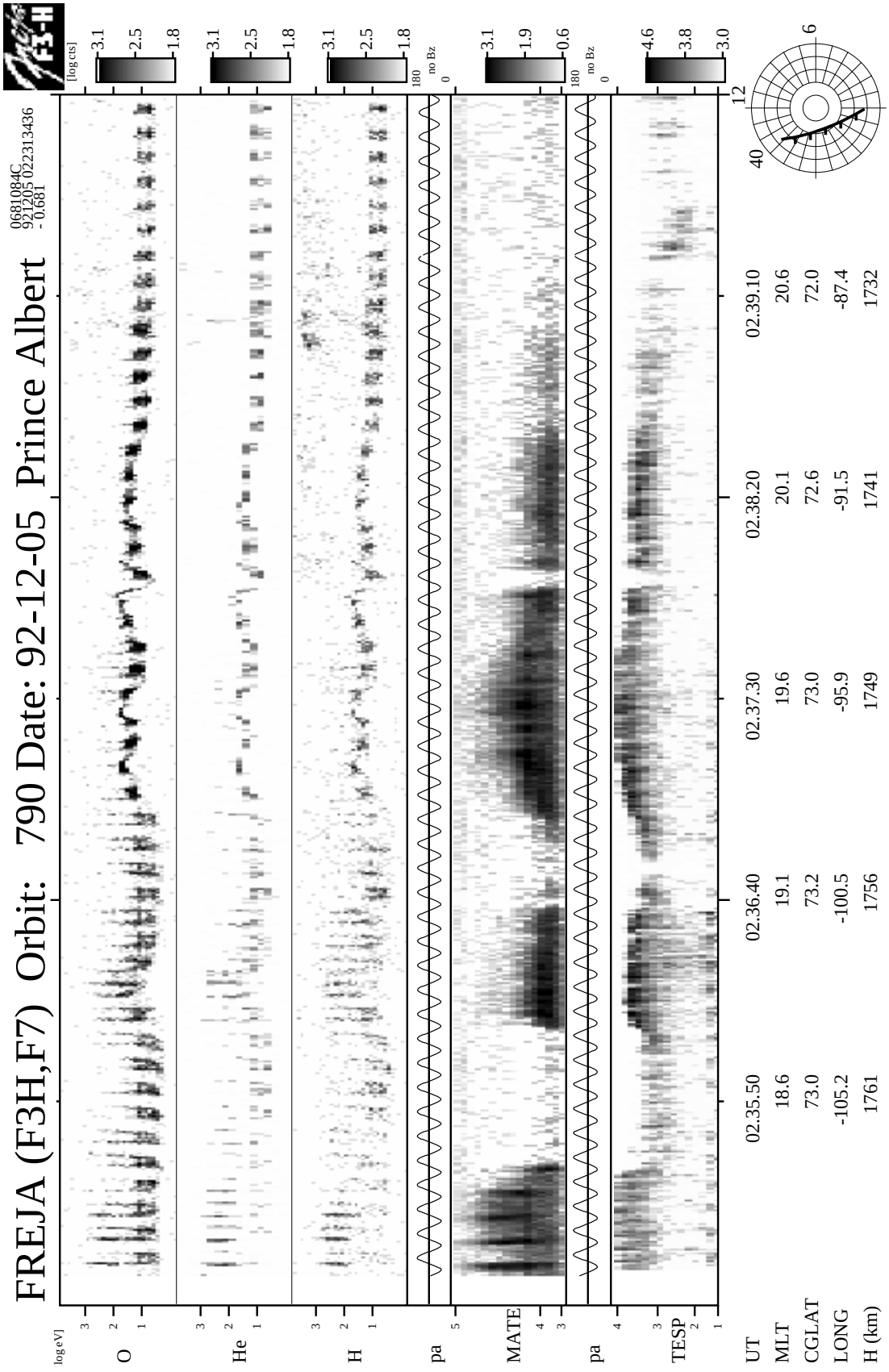

Figure 4.3-2. Orbit 790: A blowup of the particle data. A one-to-one correspondence exist between the intensity and energy of the inverted-V peak and the charging level (as detected by the uplifted energy of the ions).

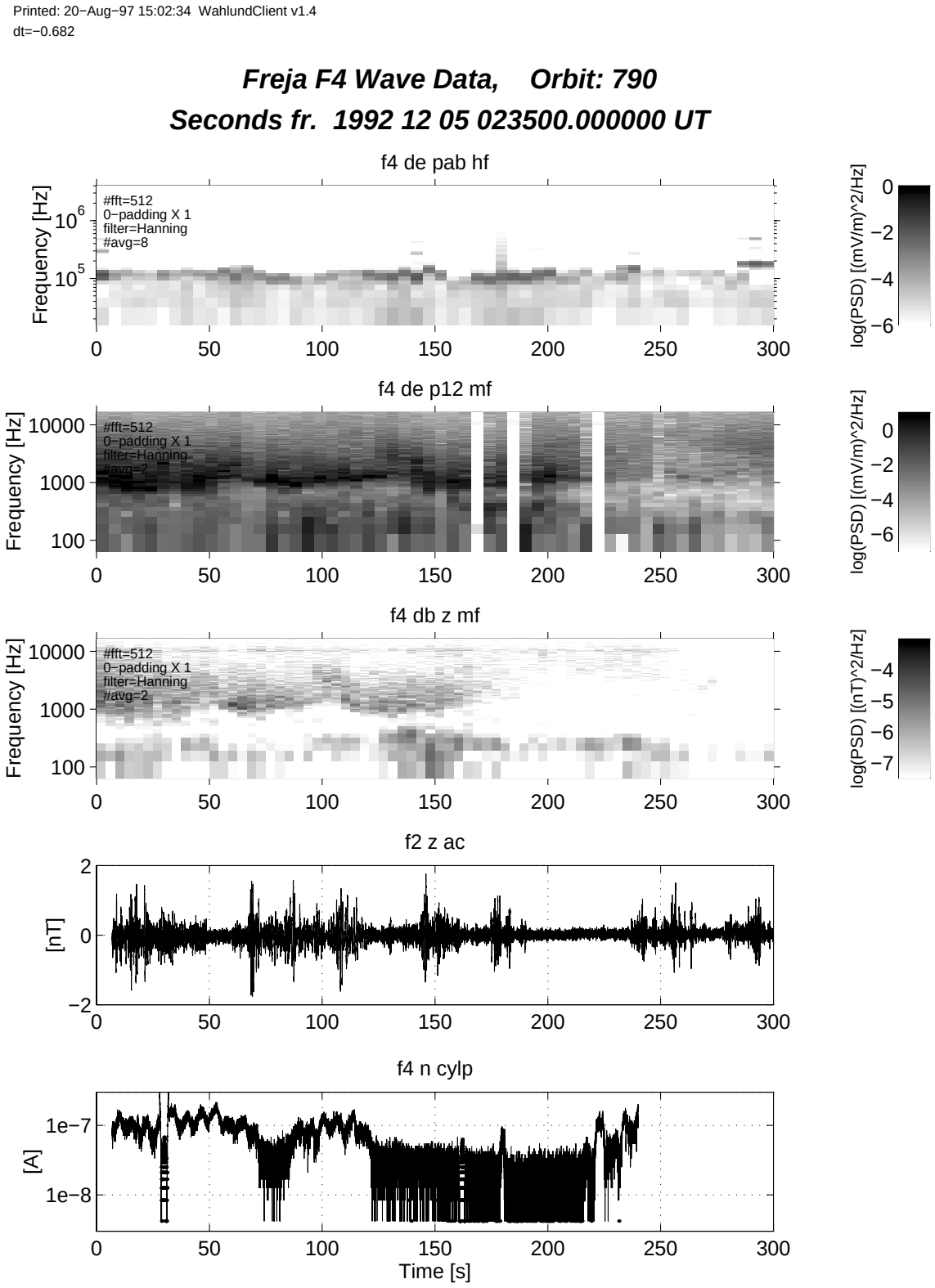

Figure 4.3-3. Orbit 790: Plasma wave data corresponding to the particle data in Figure 4.3-2. From top to bottom; HF electric data, MF electric data, MF search coil data, FGM time series, and Langmuir probe current (CYLP).

The estimated density from the HF narrowband emissions (Figure 4.3-3, panel 1) was rather constant for the whole displayed interval and attained values close to $1.2–2.8 \cdot 10^8$ m^{-3}, while the CYLP current (panel 5) occasionally dropped to very low values. Spacecraft charging is therefore suggested during the current drops. The ions were uplifted in energy to almost 100 eV (Figure 4.3-2, panels 1-3) during the CYLP current dropouts, and enhanced fluxes of high energy electrons (panels 5 and 7) correlated well in both flux intensity and maximum energy. We interpret these results that the electron flux and peak energy are major factors determining the charging level for a given plasma density.

A series of TESP are presented in Figures 4.3-4a –c, which together cover the time period 0236:40–0238:10 UT. For corresponding MATE spectra see WP-110-TN. Note how the spectra evolved with time when the charging event started, reached its maximum, and then relaxed. The maximum of the inverted-V peak reached large energies up to 10 keV during maximum charging, where also the largest electron fluxes at the highest energies occurred. The precipitating electron fluxes were close to isotropic and belonged to an inverted-V event. Thus, during the charging event the maximum flux of energetic electrons at the peak moved above the crossover energies of ITOC (2.5–3 keV) and the thermal blanket (just below 4 keV, see section 4.5. below). This suggests that the flux of the emitted secondary electrons could no longer balance the incident energetic electron flux, and in this way caused the observed negative charging. Also, the flux levels in the high energy tail up to 60 keV increased with about an order of magnitude, which further contributed to the excess charge accumulation.

Ion distributions around maximum charging are displayed in Figure 4.3-5a. They show the typical energy-lifted all-pitch-angle distribution of a charging event up to –65 V. Some indications of simultaneously occurring ion conics can be seen around 90° pitch-angle. For comparison, ion distributions from the ion conic event preceeding the charging event, are presented in Figure 4.3-5b, where clear ion conics with energies up to 1.5 keV can be seen.

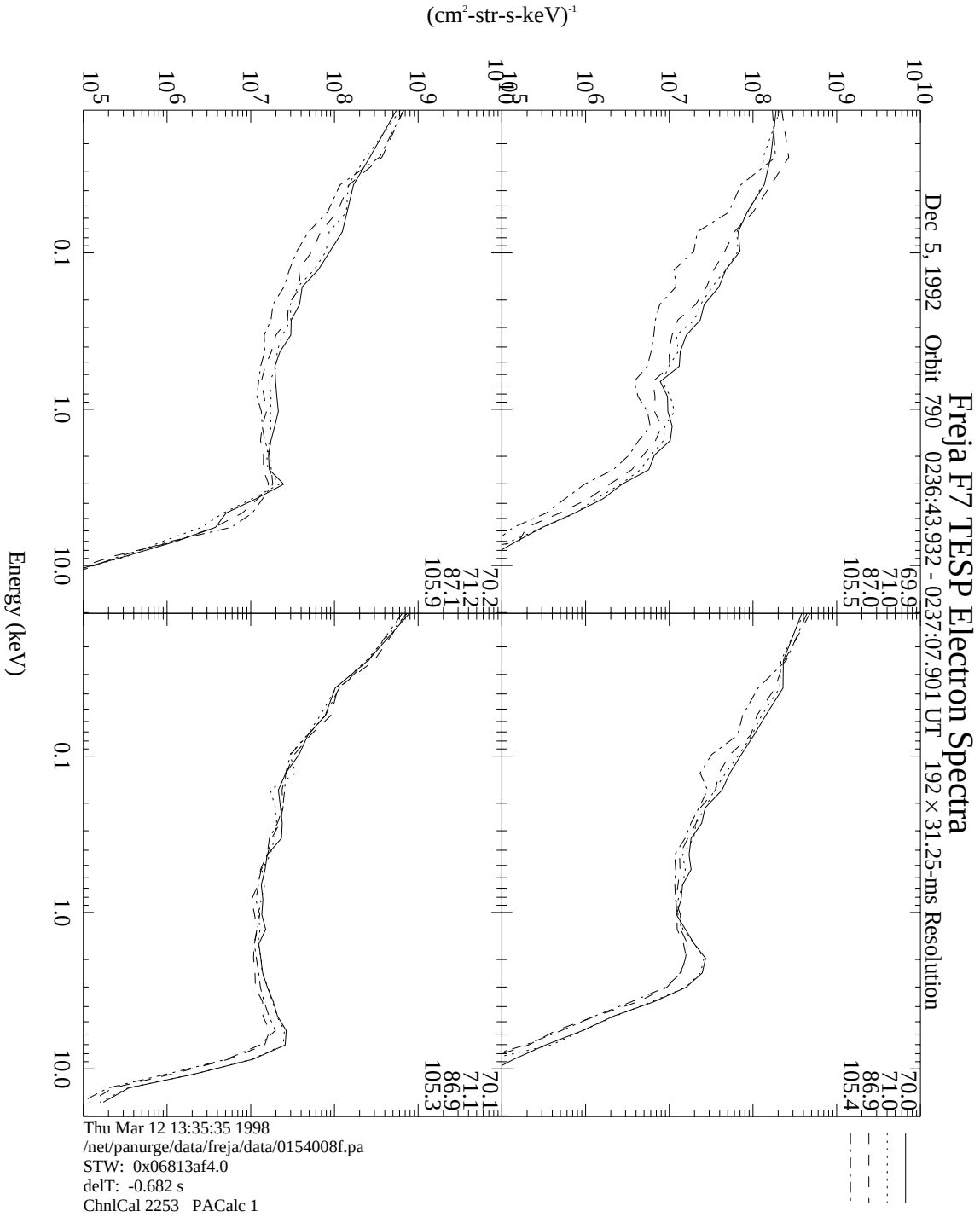

Figure 4.3-4a. Orbit 790: TESP electron spectra. Significant charging started to occur at a time corresponding to panel 4, when the inverted-V peak energy have risen above a few keV.

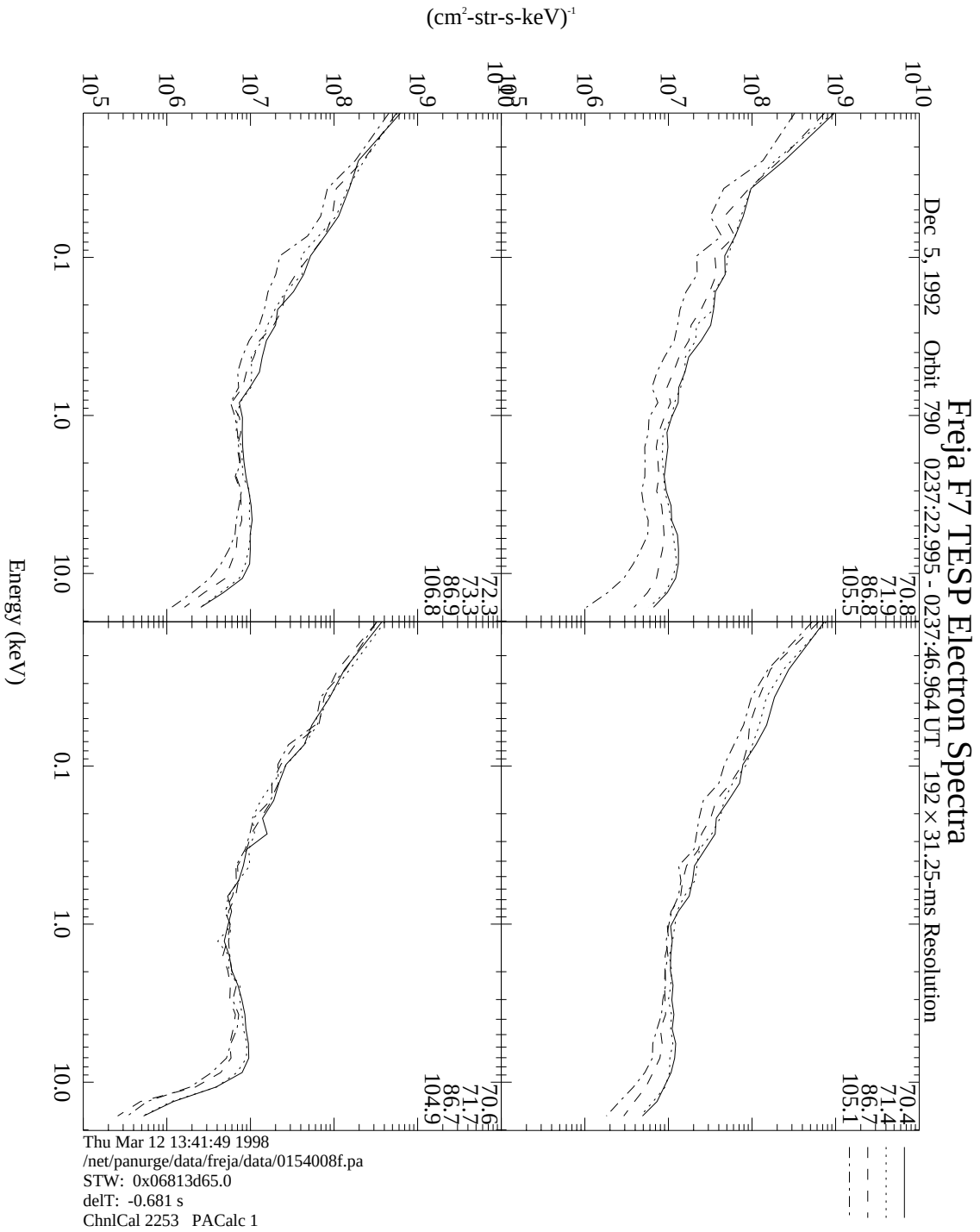

Figure 4.3-4b. Orbit 790: TESP electron spectra from a charging event.

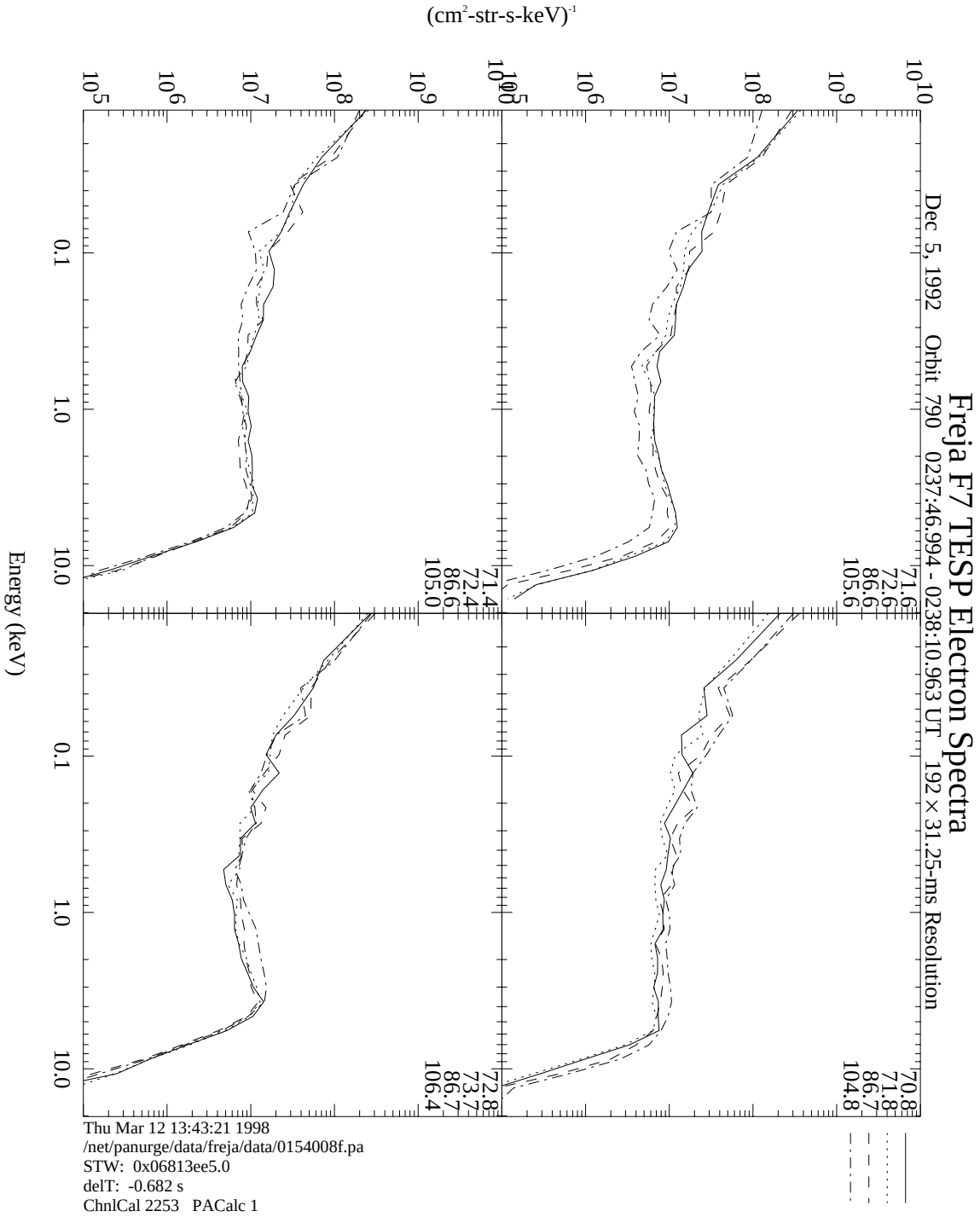

Figure 4.3-4c. Orbit 790: TESP electron spectra from a charging event.

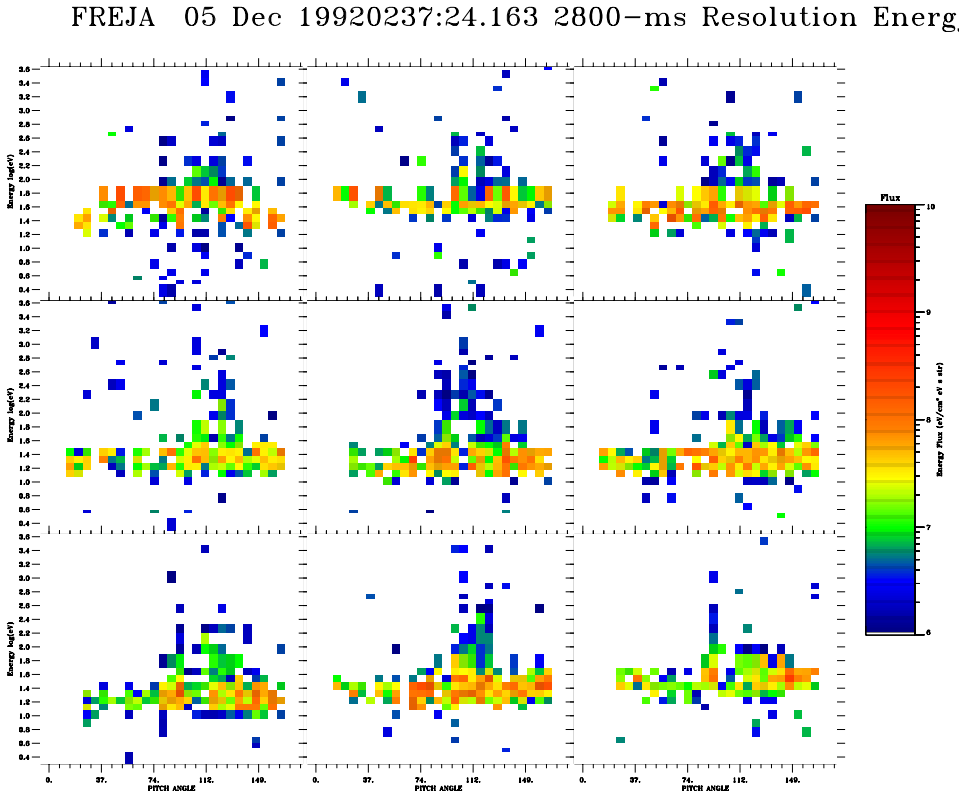

Figure 4.3-5a. Orbit 790: Ion distributions around maximum charging. They show the typical energy lifted all-pitch-angle distribution of a charging events up to –65 V.

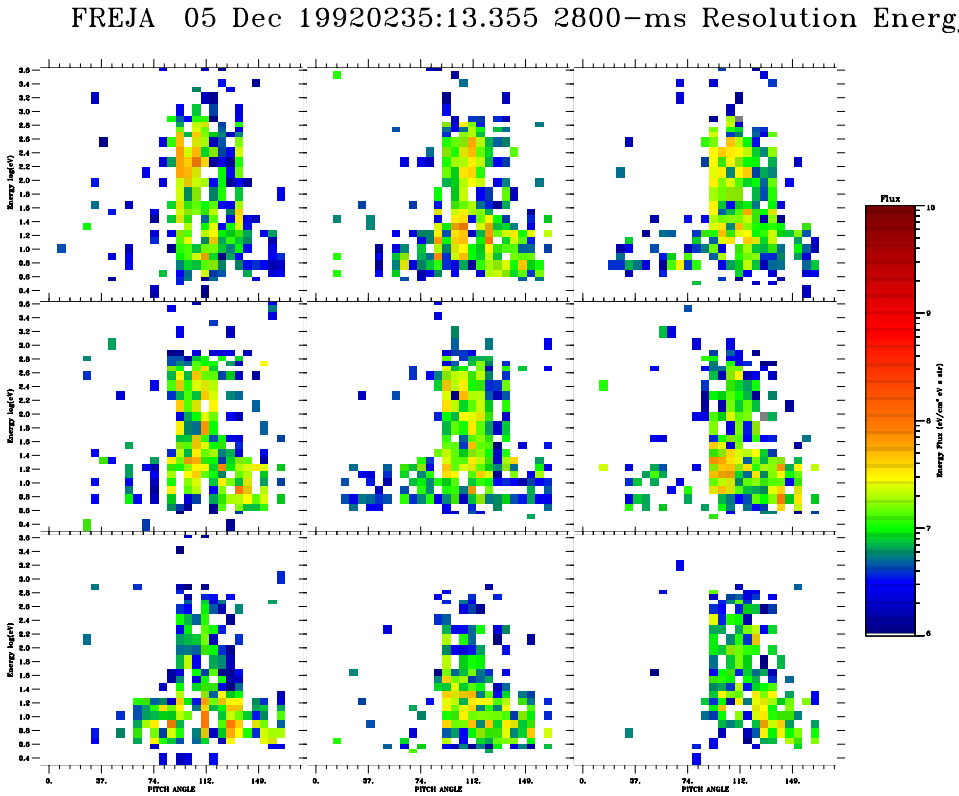

Figure 4.3-5b. Orbit 790: Ion distributions from the ion conic event preceeding the charging event. 4.3.4. Orbit 1666, one of the largest charging potentials

4.3.4. Orbit 1666, one of the largest charging potentials

The overview data for the particle measurements from orbit 1666 are presented in Figure 4.3-6. This event represents one of the largest observed charging levels observed in the Freja dataset. The ions are lifted in energy between 0916:00–0919:00 UT (panels 1-3). The event is associated with enhanced fluxes of high energy electrons which are part of an inverted-V (panel 7). The whole event occurred during eclipse (panel 4). The MATE measured only the integrated flux during this orbit.

Figures 4.3-7 and 4.3-8 display the blowup of the particle and plasma wave data around the uplifted ion event. Densities during the charging event varied between $1\text{-}2\cdot10^8$ m^{-3} according to the upper cutoff of the HF emissions (panel 1, Figure 4.3-8). In this case the thermal plasma density indeed did decrease when the charging event appeared, which was not the usual case during other charging events in the Freja dataset. The ion energy attained values up to about –2000 V near 0918:00 UT (panel 1, Figure 4.3-7), a time when the energetic electron fluxes became as most intense and the peak energy rose to its largest value (panels 5 and 7, Figure 4.3-7).

Detailed TESP spectra during the event are displayed in Figures 4.3-9a and 4.3-9b. The inverted-V peak became displaced upward in energy during maximum charging, and the peak energy was probably even above maximum measured energy (25 keV). The peak flux, on the other hand, stayed rather constant during the event. The last panel in Figure 4.3-9b, which is from the time after the charging, shows evidence of field-aligned suprathermal electron bursts in the energy range 30–1000 eV.

4.3.5. Conclusions of the detailed study of Freja charging events

More details of these and the other 8 events studied in this investigation can be found in the Technical note SPEE-WP110-TN, which is available through the www-server http://www.geo.fmi.fi/spee/docs/

The following observational conclusions can be made from the detailed study regarding surface charging on the Freja spacecraft:

- All detected charging events were related to the presence of auroral inverted-V energetic electrons, at least down to time scales of the order of 1 s.
- Charging levels up to –2000 V have been observed in eclipse although the main coating material, Indium Tin Oxide (ITO), is known to have high secondary electron emission properties.
- There is a clear proportionality between charging level and the rise of the energetic electron peak energy (and the electron flux is most often enhanced an order of magnitude at the peak energy). The highest level charging events have the highest energy peaks and fluxes.
- A high energy tail up to at least 80 keV is observed during the charging events. In some cases large fluxes of MeV electrons occurred simultaneously as inferred from the contamination of the ion measurements. Such MeV electron population

only appears during the most extreme charging events and most probably is an extension of the enhanced high energy tail. MeV electrons could penetrate the upper surface layers and possibly cause internal charging.

- A threshold energy for the inverted-V peak of about 5 keV is inferred, while no charging developed below this value. Even the low level charging events of just a few volts negative were associated with energetic electrons above this threshold.
- Most charging events occurred during eclipse, but a few took place during sunlight conditions. The peak energy threshold was larger (> 10–15 keV) during sunlight conditions.
- There is only weak indication that low energy suprathermal electron bursts below 1 keV could have inhibited charging on Freja.
- The thermal plasma density did not usually change significantly when Freja encountered a charging event as compared to the surrounding densities. Also, there is only weak indication (from orbit 736) that the thermal plasma density affected the charging levels significantly.
- Thermal plasma density was rather low ($< 10^9$ m^{-3}) during charging events.
- Several of the plasma instruments showed serious operation disturbances during high level charging events (above a few tens of volts negative). The Langmuir probe currents dropped to almost zero current due to the fact that few thermal electrons reached the probes. The same effect made the LF and MF plasma wave measurements impossible, and the TICS instrument showed almost ring distributed ions due to the fact that the ions were accelerated toward the spacecraft. In some events some plasma instruments just stopped working properly after a high-level charging event.
- Transverse ion heating show similar characteristics in the ion spectrometer data (TICS) as those during a charging event. Only careful analysis or a trained eye can easily differ between the two interpretations.
- No arcing or EMC problems have been identified during the charging events presumably because most of the spacecraft was very conductive.

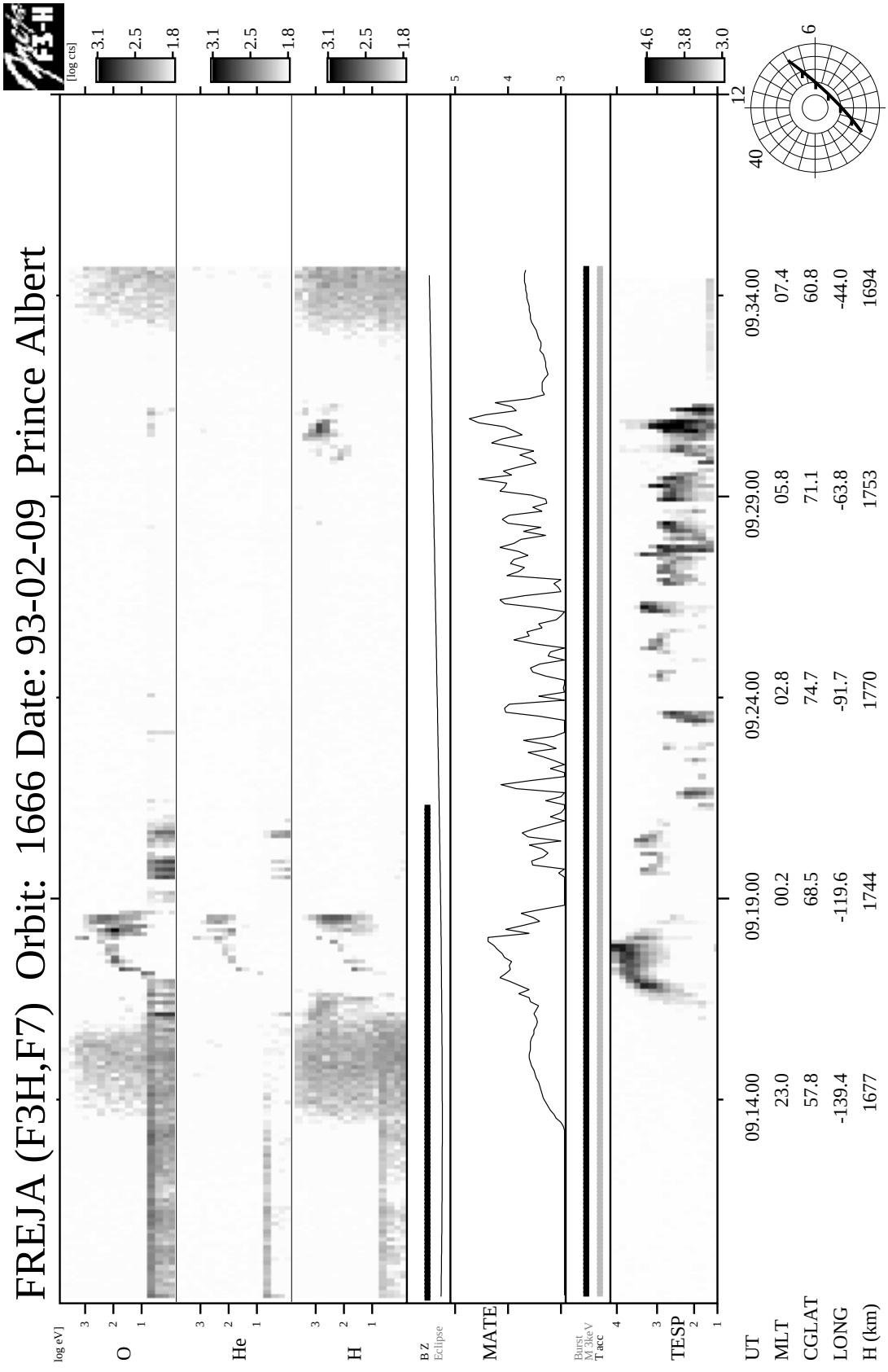

Figure 4.3-6. Overview of orbit 1666 particle data. This event represents one of the largest observed charging levels in the Freja dataset. It occurred during an intense auroral inverted-V event.

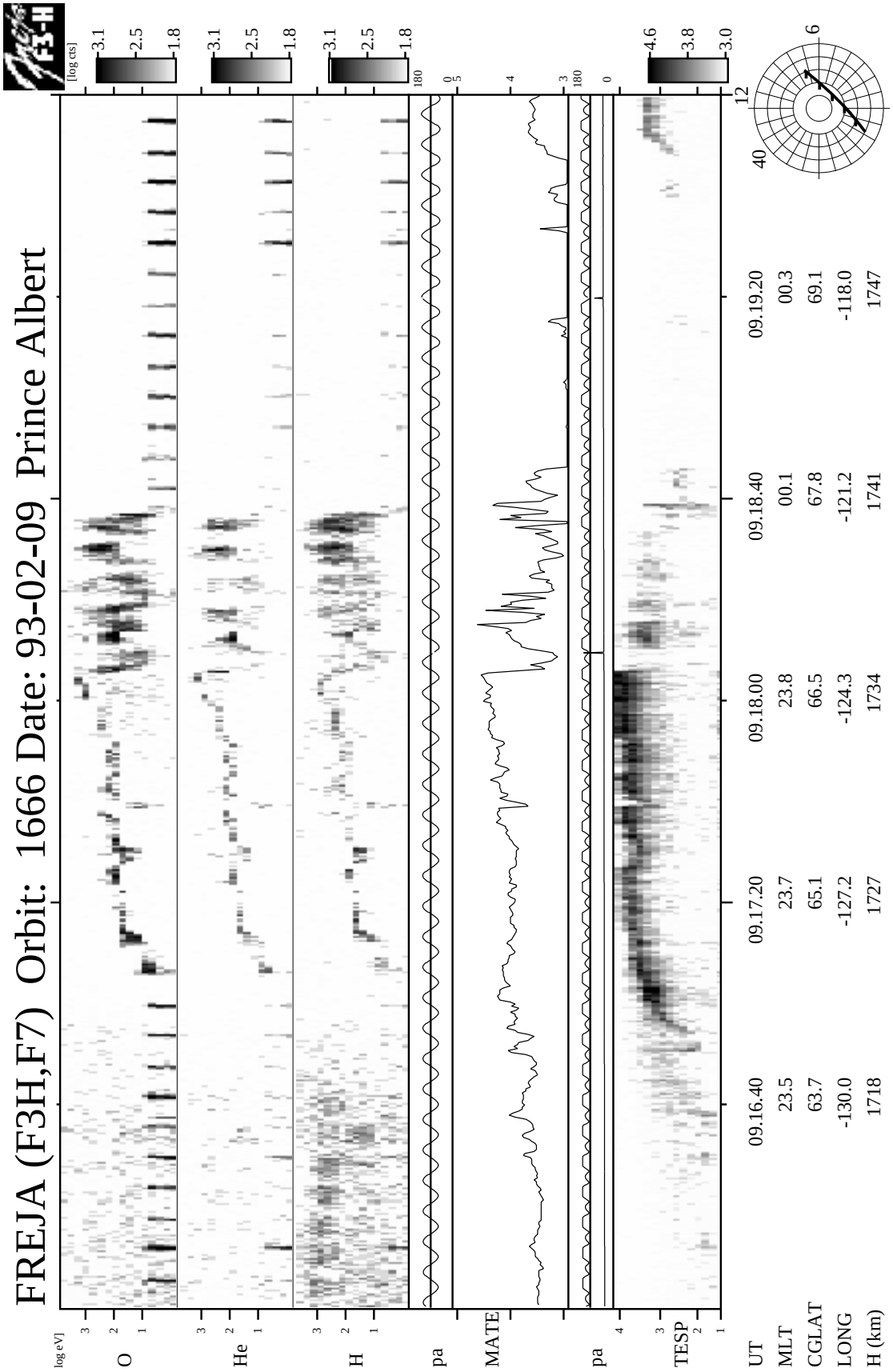

Figure 4.3-7. Orbit 1666: A blowup of the particle data. A trained eye can sort out the difference in the TICS ion data between the charging event (around 0917:00–0918:00 UT) and the later on occuring transverse ion heating event.

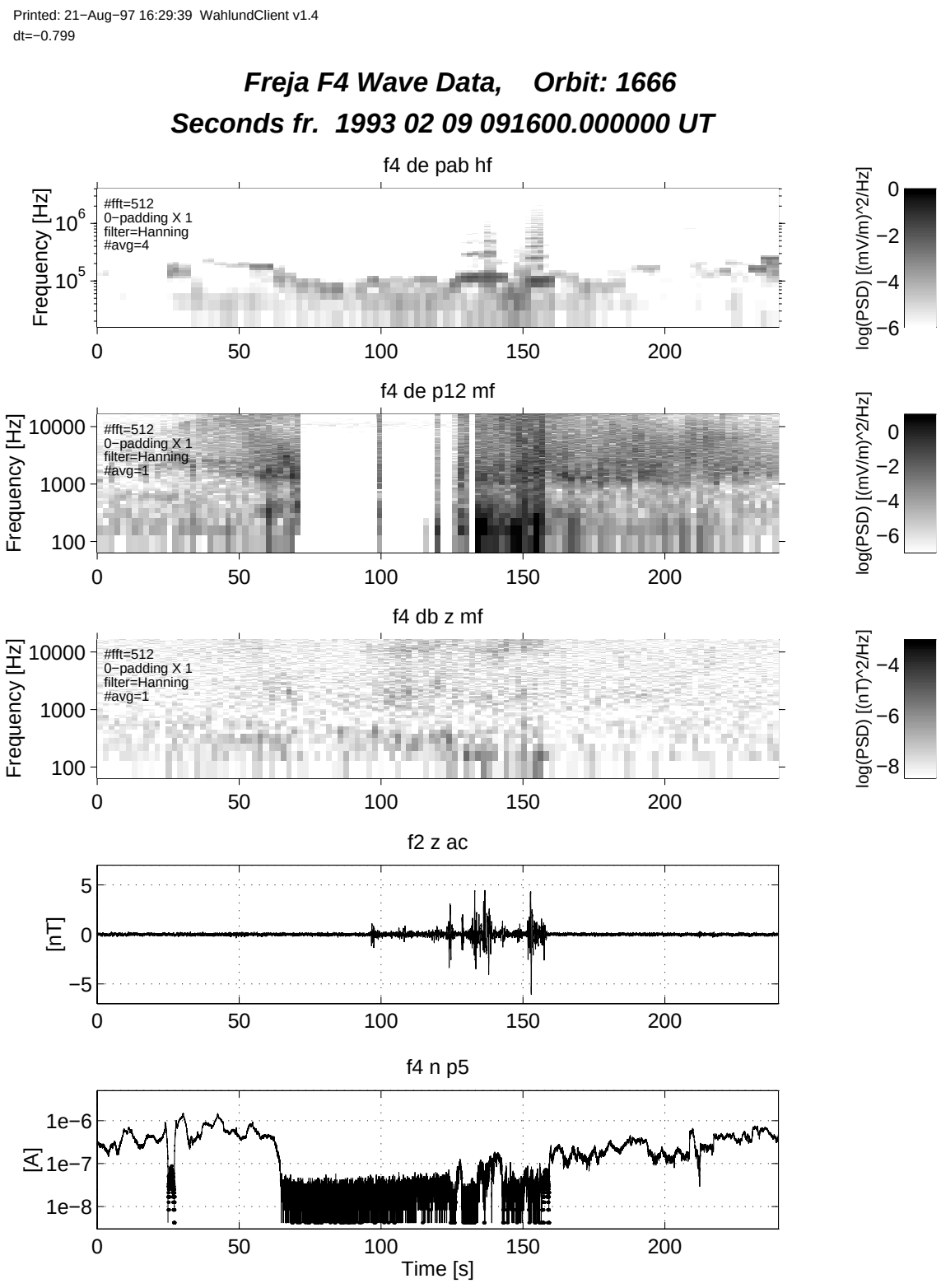

Figure 4.3-8. Orbit 1666: Plasma wave data corresponding to the particle data in Figure 4.3-7.

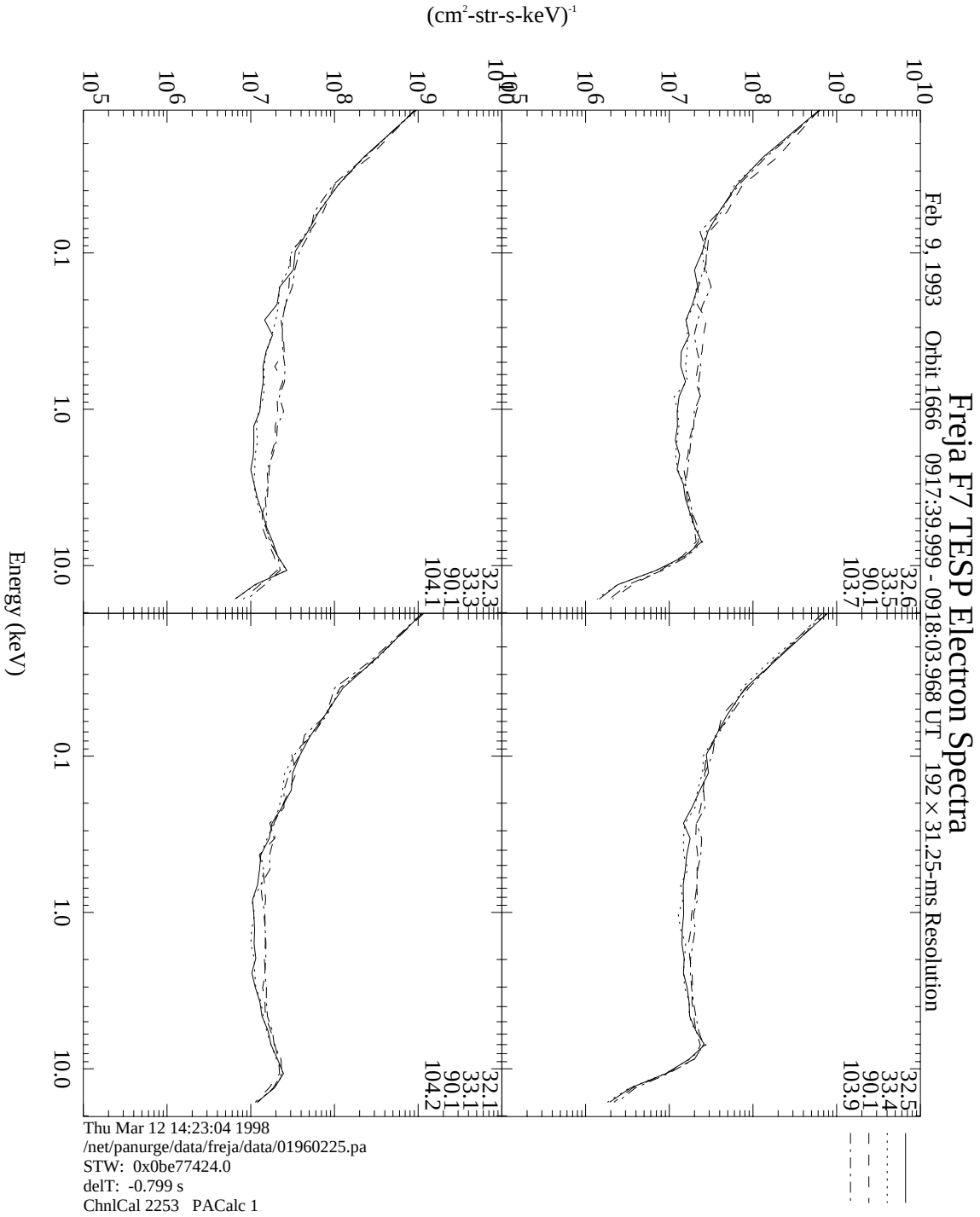

Figure 4.3-9a. Orbit 1666: Detailed TESP spectra during the charging event. The inverted-V peak becomes displaced upward in energy during maximum charging.

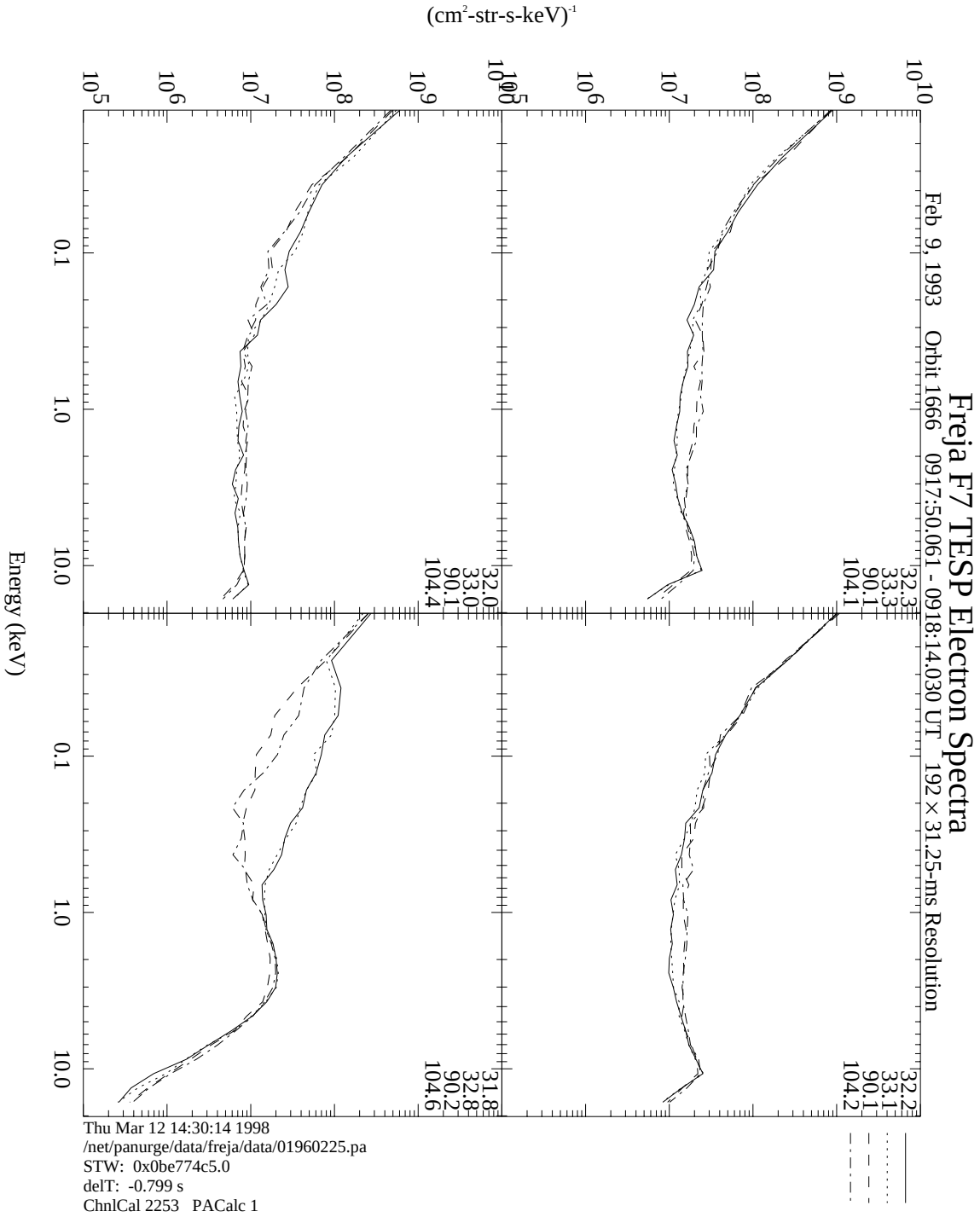

Figure 4.3-9b: Orbit 1666: A continuation of Figure 4.3-9a.